The Single Transmembrane Segment of gp210 Is Sufficient for Sorting to the Pore Membrane Domain of the Nuclear Envelope

Richard W. Wozniak and Günter Blobel

Laboratory of Cell Biology, Howard Hughes Medical Institute, The Rockefeller University, New York, New York, 10021

Abstract. The glycoprotein gp210 is located in the "pore membrane," a specialized domain of the nuclear envelope to which the nuclear pore complex (NPC) is anchored. gp210 contains a large cisternal domain, a single transmembrane segment (TM), and a COOH-terminal, 58-amino acid residue cytoplasmic tail (CT) (Wozniak, R. W., E. Bartnik, and G. Blobel. 1989. *J. Cell Biol.* 108:2083–2092; Greber, U. F., A. Senior, and L. Gerace. 1990. *EMBO (Eur. Mol. Biol. Organ.) J.* 9:1495–1502). To locate determinants for sorting of gp210 to the pore membrane, we constructed various cDNAs coding for wild-type, mutant, and chimeric gp210, and monitored localization of the expressed protein in 3T3 cells by immunofluorescence microscopy using appropriate antibodies. The large cisternal domain of gp210 (95% of its mass) did not reveal any sorting determinants. Surprisingly, the TM of gp210 is sufficient for sorting to the pore membrane. The CT also contains a sorting determinant, but it is weaker than that of the TM. We propose specific lateral association of the transmembrane helices of two proteins to yield either a gp210 homodimer or a heterodimer of gp210 and another protein. The cytoplasmically oriented tails of these dimers may bind cooperatively to the adjacent NPCs. In addition, we demonstrate that gp210 co-localizes with cytoplasmically dispersed nucleoporins, suggesting a cytoplasmic association of these components.

THE nuclear envelope (NE)[1] consists of three morphologically and biochemically distinct domains (for review see 9, 12). The outer nuclear membrane domain contains bound ribosomes and is continuous with and biochemically indistinguishable from the RER. The inner nuclear membrane domain is adjacent to the nuclear lamina and the underlying chromatin, and contains a distinct set of integral membrane proteins (1, 29, 36). Finally, the outer and inner membranes of the NE are connected with each other at numerous sites forming circular openings in the NE (nuclear pores) of ~100 nm diam. The connecting membrane is sharply bent (180°), and is referred to as the "pore membrane" domain of the NE. The nuclear pore is occupied by the nuclear pore complex (NPC) and the pore membrane is adjacent to the NPC (for review see 9, 21). The pore membrane contains at least one distinct glycoprotein, referred to as gp210 (10, 37). This, and perhaps other yet to be identified pore membrane–specific integral proteins, may function in nuclear pore formation and in the assembly and attachment of the NPC to the pore membrane.

Gp210 has been estimated to be present in 16–24 copies per nuclear pore (9). Its primary structure has been deduced from overlapping cDNA clones (37), and its topology has been determined using proteolytic enzymes and domain-specific antibodies (11; E. Bartnik, R. W. Wozniak, and G. Blobel, unpublished results). gp210 has an estimated mass of ~210,000 D, 5% of which consists of N-linked, high mannose–type oligosaccharides (2, 37). The deduced primary structure reveals an NH_2-terminal, cleaved signal sequence of 25 residues followed by 1,861 residues of the mature gp210. The NH_2-terminal 1,783 residues of mature gp210 are exposed on the intracisternal side of the pore membrane. This is followed by a transmembrane segment (TM) of 21 residues and a COOH-terminal tail of 58 residues. The tail is exposed at the nuclear pore and is therefore a potential anchor for components of the NPC.

How is gp210 sorted to the pore membrane after its signal- and stop-transfer sequence–mediated integration into the RER and the outer nuclear membrane? Like resident integral proteins of the RER and the NE, gp210 is designed to resist bulk flow from the RER into downstream membranes of the exocytotic pathway. In addition, it is sorted specifically to the pore membrane of the NE. Retention in the ER of a number of resident integral proteins, both endogenous and viral, has been shown to be mediated by sequences in the cytoplasmically exposed domains of these proteins (13, 24, 26). Because of its likely interaction with the NPC, the cytoplasmically exposed tail of gp210 seemed a likely candidate to be the determinant for sorting to the pore membrane. However, using various mutant forms of gp210, we found that its TM is sufficient for sorting to the pore membrane. The cytoplasmic tail (CT) serves as an additional, but weaker, sorting determinant.

1. *Abbreviations used in this paper*: CT, cytoplasmic tail; HA, hemagglutinin; NE, nuclear envelope; NPC, nuclear pore complex; PCR, polymerase chain reaction; TM, transmembrane segment.

Materials and Methods

Construction of a Full-Length gp210 cDNA

The cDNA sequence of rat gp210 has been previously determined from a series of overlapping, partial cDNA clones (37). To assemble a full-length cDNA molecule encoding rat gp210, we used the polymerase chain reaction (PCR) to synthesize three independent cDNAs each representing approximately one-third of the 5,658-nucleotide coding region: a 5′ fragment (nucleotides −12–1,997), a middle fragment (nucleotides 1,988–3,854), and a 3′ fragment (nucleotides 3,845–5,708). The templates used for amplification were the partial cDNA clones. Oligonucleotide primers were designed on the basis of the published cDNA sequence of gp210.

Synthesis of the 5′ fragment was complicated by the lack of a complete template encoding this region. To circumvent this problem, inserts from three overlapping, partial cDNA clones, which together span this region, 50–17, 45–A1, and 47–10 (37), were used to synthesize a hybrid cDNA of sufficient length to act as a template for amplification. Synthesis of this template was performed as follows. Two overlapping cDNA clones, 50–17 and 45–A1 (~50 ng each), were cleaved with EcoRI and XhoI, respectively, to liberate two overlapping inserts. The resulting DNA fragments were combined and heat denatured at 95°C for 10 min in 1× Taq polymerase buffer (Perkin-Elmer Cetus Instruments, Norwalk, CT). The denatured DNA was allowed to reanneal at 65°C for 30 min and dATP, dCTP, dGTP, and dTTP were added to a final concentration of 0.2 mM each. The reaction temperature was raised to 72°C and 2.5 U of Taq polymerase (Perkin Elmer Cetus Instruments) was added to fill in the fraction of DNA molecules formed by the hybridization of overlapping single-stranded inserts from 50–17 and 45–A1. The polymerization was allowed to proceed for 8 min at 72°C. The DNA from this reaction, containing the double-stranded 50–17/45–A1 hybrid, was combined with ~50 ng of EcoRI/AatII cut 47–10 cDNA, and the denaturation, annealing, and polymerization steps repeated as above to form a 50–17/45–A1/47–10 hybrid cDNA. Although this species likely represents only a fraction of the total cDNA present in the reaction, it proved sufficient for amplification. With this template, a PCR was performed using a sense oligonucleotide encoding a 5′ SalI site followed by nucleotides −12–33 (sense primer) and an antisense oligonucleotide encoding nucleotides 1,967–1,997 (antisense primer).

Two additional PCR products were synthesized encoding the remaining two-thirds of the full-length cDNA. The middle segment was synthesized using the cDNA clone 47–11 as a template and oligonucleotide primers encoding nucleotides 1,937–2,016 (sense) and nucleotides 3,826–3,854 (antisense). The 3′ segment was synthesized using the cDNA clone 49–10 as a template and oligonucleotide primers encoding nucleotides 3,845–3,873 (sense) and nucleotides 5,664–5,708 plus a 5′ SalI site (antisense). Point mutations were introduced at nucleotide positions 1,992 and 3,849 of the above oligonucleotide primers to create two unique BstBI sites at positions 1,990 and 3,847 without altering the amino acid sequence of gp210. These sites were used to assemble a full-length gp210 cDNA with flanking, unique SalI sites. Sequencing of this clone revealed four nucleotide changes produced during the PCR reactions. Two of these led to changes in the amino acid sequence, one at position 491 (serine to glycine) and the other at position 1,131 (leucine to histidine).

Epitope Tagging of gp210

To distinguish the expression of recombinant gp210 from the endogenous protein, an epitope tag encoding a 12-amino acid residue peptide from the influenza virus HA molecule (8, 34), with two flanking glycine residues added as spacers, was inserted into gp210 after amino acid residue 28. This was accomplished by synthesizing two complimentary oligonucleotides, HA-1 and HA-2, with the following sequence.

```
5′ ag cta ggt tac cca tac gat gtt cca gat tac gct agc ttg ggt a 3′      HA-1
   3′ t cca atg ggt atg cta caa ggt cta atg cga tcg aac cca ttc ga 5′  HA-2
      G  Y  P  Y  D  V  P  D  Y  A  S  L  G      amino acid
                                                 residues
```

This oligonucleotide pair was inserted into a HindIII site (nucleotide 79) of the gp210 cDNA. The orientation of the insert and the reading frame of the resulting gp210:HA cDNA was confirmed by DNA sequencing. The gp210:HA cDNA was subcloned into the XhoI site of the eukaryotic expression vector pSVL (Pharmacia LKB Biotechnology, Piscataway, NJ).

Construction of the gp210-(TM + CT):HA Deletion Mutant

Deletion of the TM and the CT of gp210 was achieved by inserting a stop codon after nucleotide 5,424 into the gp210:HA cDNA. This was accomplished by inserting a PCR product into a unique BglII site at nucleotide 5,139. This PCR product is identical to the gp210 cDNA from the BglII site downstream to the codon for amino acid residue 1,808, after which a stop codon is inserted. It was synthesized using the cDNA clone 49–10 as a template and two oligonucleotide primers, a sense primer encoding nucleotides 5,125–5,141 and an antisense primer encoding nucleotides 5,409–5,424 followed by an in-frame stop codon and a 5′ BglII linker. After cleavage with BglII, the PCR product was introduced into the gp210:HA reading frame at the BglII site. The orientation and the reading frame of the insert were determined by DNA sequencing. This gp210-(TM + CT):HA mutant (see Fig. 1) was inserted into the pSVL plasmid for expression studies.

Construction of Expression Plasmids Containing CD8 and CD8/gp210 Chimeric cDNAs

Expression of the wild-type CD8 cDNA was accomplished as follows. A pSP65 plasmid containing the F1 cDNA clone of CD8 (18) (pSP65F1, kindly provided by Dr. Giovanni Migliaccio, Istituto di Ricerche di Biologia Molecolare, Pomezia, Italy) was digested with EcoRI to remove the full-length CD8 cDNA. The cohesive ends were filled in with Klenow fragment and the cDNA was subcloned into the SmaI site of the pSVL plasmid for expression studies.

Chimeric cDNAs encoding the fusion proteins CD8/gp(TM + CT), CD8/gp(TM + CT)-20, and CD8/gp(TM + CT)-54 (see Fig. 1) were constructed as follows. pSP65F1 was digested with XbaI and EcoRV to produce a DNA fragment containing nucleotides 1–611 of the CD8 cDNA (18). The 3′ blunt-end site created by EcoRV follows the codon for amino acid residue 161 (18). This fragment was combined separately with each of three PCR products that encode amino acid residues 1,806–1,886 (CD8/gp[TM + CT]), 1,806–1,866 (CD8/gp[TM + CT]-20), or 1,806–1,822 (CD8/gp[TM + CT]-54) of gp210 (see Fig. 1). In each PCR product the gp210 coding region is followed by a 3′ termination codon and a BamHI linker. The CD8 cDNA fragment was blunt-end ligated to each of the PCR products to produce the appropriate chimeric cDNA and subcloned into a XbaI and BamHI cut pSVL plasmid.

The assembly of the CD8/gpCT and CD8/gpCT-20 chimeric constructs (see Fig. 1) was performed by similar methods with the following exceptions. The CD8 portion of the molecule was contributed by a PCR product that begins at a XbaI site in pSP65F1 upstream of the CD8 cDNA and continues through CD8 to nucleotide 692. The PCR product encoding the gp210 CT and the 20-amino acid deletion both begin with nucleotide 5,485 and end with a termination codon and a BamHI linker after nucleotide 5,664 (CD8/gpCT) or nucleotide 5,598 (CD8/gpCT-20). The PCR product derived from the CD8 cDNA was blunt-end ligated to each of the gp210 PCR products to produce the appropriate chimeric cDNAs which were subcloned using their flanking XbaI and BamHI sites into the pSVL expression plasmid. The structure of all of the above mutants was confirmed by DNA sequencing. The CD8/E19 chimeric cDNA within the pCMUIV plasmid (24) was kindly provided by Dr. Stefano Bonatti (Università di Napoli, Napoli, Italy) with permission from Dr. Per Peterson (Scripps Clinic, La Jolla, CA).

Expression of Recombinant cDNAs in Mouse Balb/c 3T3 Fibroblasts

The expression of chimeric proteins in mouse Balb/c 3T3 cells was accomplished by direct microinjection of plasmid DNA into nuclei using a procedure described by Capecchi (5). Subconfluent cultures of Balb/c 3T3 cells were grown on 12-mm diam. glass coverslips in DME medium (Gibco Laboratories, Grand Island, NY) supplemented with 10% FBS (Gibco Laboratories), 20 mM Hepes, pH 7.4, and 50 μg/ml Gentamycin (Gibco Laboratories). Nuclei were injected with plasmid DNA purified using a plasmid purification kit (Qiagen Inc., Chatsworth, CA) at 1 mg/ml in PBS containing 1 mM $MgCl_2$. The microinjection equipment consisted of an Eppendorf injector 5,242 and a Zeiss micromanipulator MR mounted on a Zeiss Axiovert 10 microscope (Zeiss, Oberkochen, Germany). After injection, the cells were returned to a 5% CO_2 incubator at 37°C for 4–5 h.

Immunofluorescence Microscopy

Coverslips containing injected 3T3 cells were processed for immunofluores-

cence microscopy as follows. 4–5 h after injection, cells were fixed with 3% paraformaldehyde in PBS for 20 min on ice. After fixation, cells were washed with PBS and permeabilized with 0.1% Triton X-100 in PBS for 2 min on ice. Cells were then washed with PBS and nonspecific sites blocked with milk buffer (2% nonfat dry milk, 0.1% Tween 20, 40 mM K_2HPO_4, 10 mM KH_2PO_4, 150 mM NaCl, and 0.01% NaN_3) for 1–2 h at room temperature. All subsequent steps were performed at room temperature. First antibody incubations to detect epitope-tagged proteins were performed with an mAb, 12CA5 (kindly provided by Dr. Richard Lerner, Scripps Clinic, La Jolla, CA), specific for the HA peptide tag (34) (at a 1:300 dilution of ascites fluid in 1% BSA in PBS). The detection of wild-type CD8 and CD8-containing chimeric proteins was performed with an mAb, OKT8 (kindly provided by Dr. Giovanni Migliaccio, Istituto di Ricerche di Biologia Molecolare, Pomezia, Italy), directed against the extracellular domain of CD8 (at a 1:100 dilution of culture supernatant in milk buffer). First antibody incubations were performed for 40 min followed by extensive washing with milk buffer. Primary antibody reactivity was visualized with Texas red–conjugated goat anti-mouse IgG (Molecular Probes, Inc., Eugene OR) used at 10 μg/ml in milk buffer. Cells were probed for 40 min and then washed extensively with milk buffer followed by two washes with 1% BSA in PBS.

For double-immunofluorescence experiments with the NPC-specific mAb 414 (7), the expressed recombinant protein was first detected with primary and secondary antibodies as described above and then processed as follows. Cells were washed with PBS, refixed with 1% paraformaldehyde in PBS for 1 min, and washed extensively with PBS. Samples were then washed once with milk buffer and incubated for 15 min with a 1:50 dilution of mouse serum in milk buffer to block nonspecific sites. After this incubation, cells were probed for 30 min with FITC-labeled mAb 414 (kindly provided by Dr. Thomas Meier, Rockefeller University, New York, NY) in milk buffer containing a 1:100 dilution of mouse serum. Unbound antibody was removed by extensive washing with milk buffer followed by two washes with 1% BSA in PBS. For all immunofluorescence experiments, cells were mounted in 90% glycerol containing 1 mg/ml *p*-phenylenediamine and viewed with a Zeiss Axiophot microscope. Photographs were taken through a 63× or 100× objective onto Kodak (T-Max 400, Eastman Kodak Co., Rochester, NY) film push processed to 1600 ASA.

Results

After its integration into the ER membrane, gp210 is sorted to the pore membrane, most likely by lateral diffusion in the plane of the membrane. To locate the determinant(s) for sorting, we constructed various cDNAs coding for wild-type, mutant, and chimeric gp210 (Fig. 1); subcloned them into a transient eukaryotic expression vector (pSVL); injected the DNA directly into the nuclei of subconfluent, unsynchronized 3T3 cells; and monitored localization of the expressed protein by immunofluorescence microscopy using the appropriate antibodies. Typically, 100–200 cells were injected for each experiment and the location of expressed protein was assessed 4–5 h after injection. This time period was experimentally determined to be optimal as it yielded levels of expressed protein that were sufficient for immunofluorescence detection but avoided overexpression and concomitant mislocalization.

Epitope-tagged gp210:HA Is Sorted to the Pore Membrane

To distinguish the expression of recombinant from endogenous gp210, we inserted an epitope tag encoding 12-amino acid residues of HA (8, 34) after the second residue of the mature form of gp210 (see Fig. 1). Using an mAb against the tag (anti-HA antibody), the expressed gp210:HA showed the punctate distribution at the nuclear surface (Fig. 2 *A*) that is characteristic for endogenous gp210 in the pore membrane (6). To further substantiate the localization of gp210:HA in

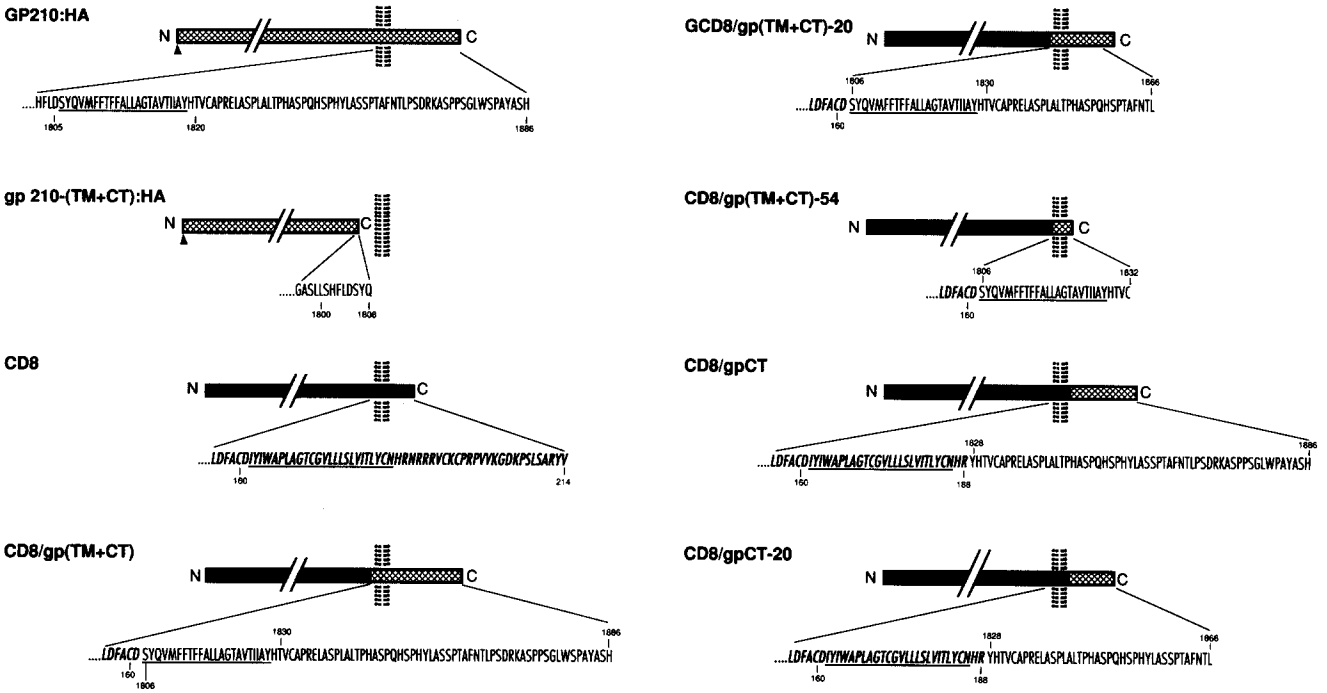

Figure 1. Schematic representations of cDNA constructs. The terms used for each construct are shown on the left. The amino terminus (*N*) and the carboxy terminus (*C*) are indicated. Segments positioned to the left of the schematic lipid bilayer lie within the lumenal or extracellular compartments and those to the right extend into the cytosol. Amino acid residues within regions of interest are listed below each schematic diagram. Those residues that span the membrane are underlined. Regions of the constructs derived from gp210 or CD8 are distinguished graphically and by print type (gp210 ▭ or *CD8* ▬). Amino acid residues are numbered in accordance with publications describing their positions within the wild-type proteins (18, 37). The arrowheads in gp210:HA and gp210-(TM + CT):HA point to the approximate position of the HA epitope tag.

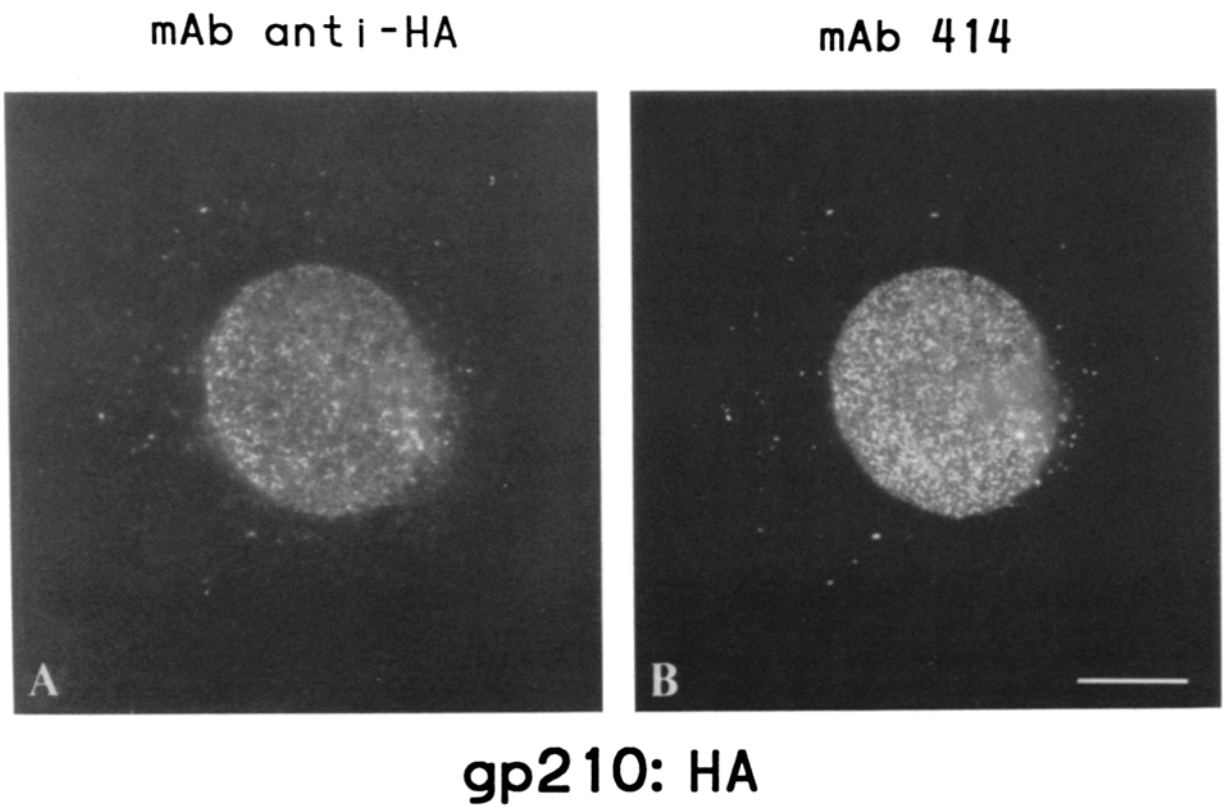

Figure 2. gp210:HA is targeted to the pore membrane domain. Cells expressing the epitope-tagged gp210:HA protein (see Fig. 1) were fixed, permeabilized, and probed with an mAb (12CA5) directed against the HA epitope tag. Binding to gp210:HA was visualized with Texas red-labeled goat anti-mouse IgG (*mAb anti-HA, A*). The locations of pore complexes within the same cell were determined by probing with a FITC-labeled mAb specific for a subset of the nucleoporins (*mAb 414, B*). The focal plane shown in *A* and *B* is tangential to the nuclear surface. gp210:HA is visible at densely packed points along the surface of the nucleus and, to a much lesser extent, in a dispersed pattern in the cytoplasm. Note the extensive coincidence between this pattern and the NPC pattern shown in *B*. Bar, 10 μm.

the pore membrane, we carried out double immunofluorescence with mAb 414 (Fig. 2 *B*). This mAb reacts with several nucleoporins (7) (all proteins of the NPC, excluding integral proteins of the pore membrane). A comparison of the two staining patterns (Fig. 2, *A* and *B*) showed considerable congruity, not only between the densely punctate pattern at the nuclear surface, but also between the more dispersed punctate pattern observed in the cytoplasm. The matching patterns in the cytoplasm suggest that gp210:HA and at least some of the nucleoporins are present as assembled structures in the ER. These structures might be similar to annulate lamellae (15). Together these data suggest that epitope tagging of gp210 does not interfere with sorting.

Gp210:HA Lacking the TM and the CT Is Not Sorted to the Pore Membrane

Having shown that gp210:HA is correctly sorted, we constructed a mutant cDNA coding for a protein that lacked both the TM and the CT, referred to as gp210-(TM + CT):HA (see Fig. 1). This protein showed a distribution characteristic of ER proteins (Fig. 3 *B*) and was no longer visible in the pore membrane, either when focusing on the nuclear surface (not shown), or when focusing on the nuclear rim (Fig. 3 *B*). Double immunofluorescence with mAb 414 did show the characteristic punctate rim pattern of the nucleoporins (Fig. 3 *A*). Likewise, a punctate nuclear rim staining pattern was seen with the anti-HA antibody in cells expressing gp210:HA (Fig. 3 *C*). We conclude that the NH_2-terminal ectoplasmic domain preceding the TM and comprising ~95% of gp210 lacks topogenic determinants for sorting to the pore membrane.

The TM of gp210 Is Sufficient for Sorting to the Pore Membrane

As the NH_2-terminal ectoplasmic domain of gp210 is not localized to the pore membrane, the topogenic determinants for pore membrane localization of gp210 must reside either in its TM, or in its CT, or in both. To distinguish between these possibilities, we constructed a cDNA coding for a chimeric protein, referred to as CD8/gp(TM + CT) (see Fig. 1) that consists of the ectoplasmic domain of CD8, used as a reporter, and the TM plus the CT of gp210. CD8 is an integral protein of the plasma membrane present in a subset of human T lymphocytes (27). Like gp210, CD8 is a bitopic integral membrane protein. Its NH_2-terminal ectoplasmic domain (161 residues) is followed by a TM and a CT (28 residues) (18, 31). After signal- and stop-transfer sequence-mediated integration into the RER, CD8 ends up, via the exocytotic pathway, in the plasma membrane. If the TM and the CT (TM + CT) portions of gp210 contain the determinants for sorting to the pore membrane, the chimera CD8/gp(TM + CT) should be localized to the pore membrane. Indeed, staining of cells expressing this fusion protein with an anti-CD8 antibody showed a characteristic punctate pore

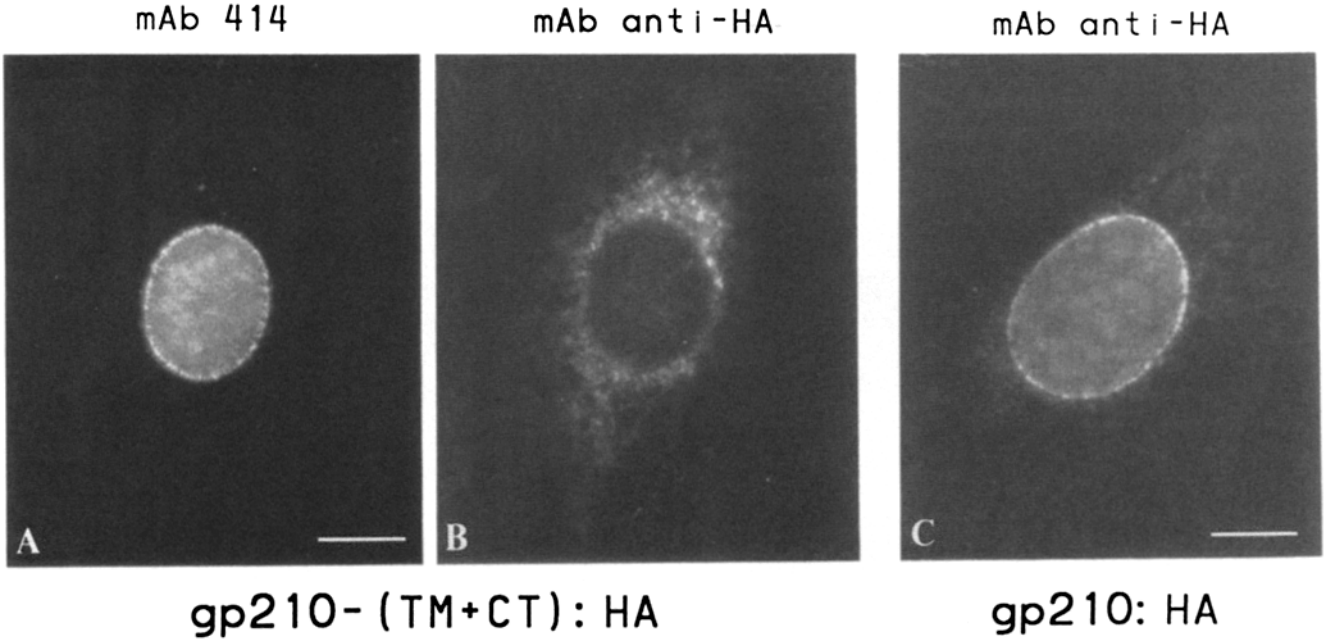

Figure 3. The targeting of gp210:HA to the pore membrane is dependent on the presence of the TM and the CT. Cells expressing the gp210-(TM + CT):HA mutant (see Fig. 1) were examined using the double-immunofluorescence procedure described in Fig. 2 to compare the localization of this chimeric protein (*mAb anti-HA*, *B*) to the position of pore complexes (*mAb 414*, *A*). For comparison, a cell expressing gp210:HA is shown in *C*. In each case, the focal plane passes through the center of the nucleus and reveals the nuclear rim. In this focal plane, pore complexes are visible as a punctate ring around the nucleus (*A*). Note the presence of the gp210-(TM + CT):HA protein in the ER (*B*) and compared this with the positions of pore complexes (*A*) and the contrasting pattern seen for gp210:HA (*C*). Bar, 10 μm.

membrane pattern at the nuclear surface and at distinct points in the cytoplasm (Fig. 4 *A*). This pattern was largely congruent with that obtained with mAb 414 (Fig. 4 *C*) in doubly stained cells. A control experiment showed wild-type CD8 to localize to the plasma membrane (Fig. 4 *B*).

To determine whether the CT domain of CD8/gp(TM + CT) is required for sorting, we prepared a series of constructs where 10, 20, 30, 43, and 54 COOH-terminal residues of the 58-residue–long CT of the CD8/gp(TM + CT) were deleted (see Fig. 1). All of these proteins were correctly sorted to the pore membrane. Only the data for the CD8/gp(TM + CT)-20 and CD8/gp(TM + CT)-54 are shown (Fig. 5). Double immunofluorescence with both the anti-CD8 antibody and mAb 414 showed that the distribution of these chimeric proteins (Fig. 5 *A* and *B*) matched that of the nucleoporins (Fig. 5, *C* and *D*). The 54-residue deletion removes nearly the entire CT leaving only four residues of the CT adjacent to the lipid bilayer. Data presented in the next section demonstrate that these four remaining residues are not sufficient for targeting to the pore membrane within the context of the CD8 TM (see Fig. 7 *B*). Therefore, at most they play an accessory role in sorting. We thus conclude that the TM of gp210 is sufficient for pore membrane localization.

The CT of gp210 Is a Sufficient, but Weak, Determinant for Sorting to the Pore Membrane

To examine whether the CT of gp210 by itself contains topogenic determinants for pore membrane localization, we prepared a chimeric construct referred to as CD8/gpCT, where the CT of CD8 was replaced with that of gp210 (see Fig. 1). Immunofluorescence with anti-CD8 antibody (Fig. 6 *B*) detected CD8/gpCT at the plasma membrane, in a densely stained region near the nucleus (presumably representing the Golgi complex), and in a punctate pattern along the nuclear rim. This punctate nuclear rim pattern of CD8/gpCT matched the nucleoporin pattern when cells were double stained with mAb 414 (Fig. 6 *A*). However, the match was less than perfect, apparently obscured by the Golgi and plasma membrane localization of CD8/gpCT. Additional support for a pore membrane localization of CD8/gpCT was provided by comparing its staining pattern with that of CD8/E19, a resident integral membrane protein of the ER (13, 24, and Fig. 6 *C*). CD8/E19 is a chimeric protein where the CT of CD8 has been replaced by the CT of E19, a viral protein that is retained in the ER (30). Although both chimeric proteins showed nuclear rim staining, only CD8/E19 additionally showed the typical ER staining pattern, indicating that the nuclear rim staining of CD8/gpCT is likely the result of localization to the pore membrane, rather than retention in the ER. Moreover, a deletion mutant of CD8/gpCT lacking 20 COOH-terminal residues from the CT (CD8/gpCT-20, see Fig. 1) is no longer localized to the pore membrane, but rather is present exclusively at the plasma membrane (Fig. 7, compare *A* and *B*). Taken together, these data suggest that the CT of gp210 contains a determinant for sorting to the pore membrane and that this determinant might reside in its COOH-terminal 20 residues.

Discussion

Most integral proteins of the membranes in the exo- and endocytotic pathway are asymmetrically integrated into the ER

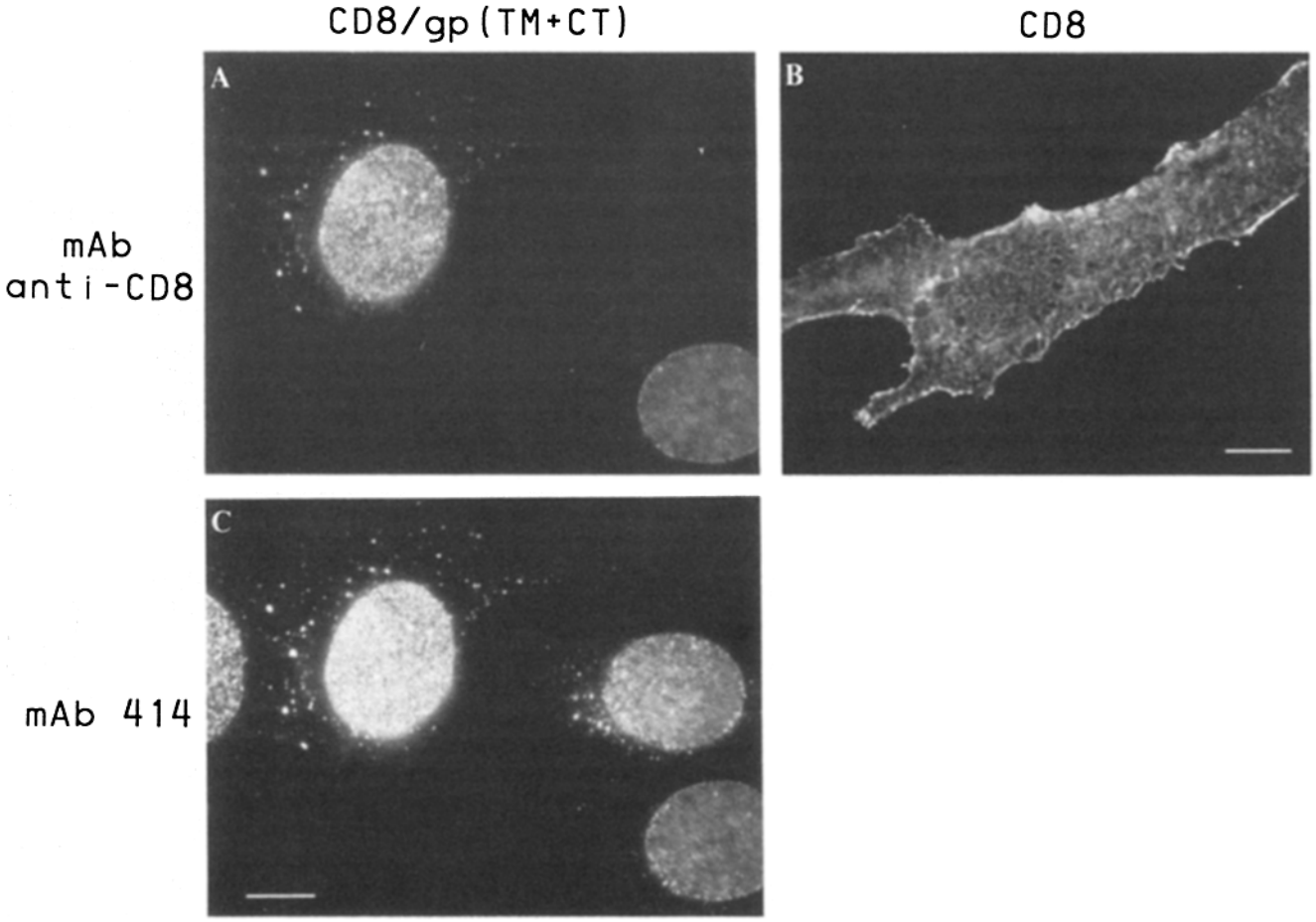

Figure 4. A reporter protein can be targeted to the pore membrane by the TM and the CT of gp210. 3T3 cells expressing the chimeric protein CD8/gp(TM + CT) (see Fig. 1), were examined by double immunofluorescence microscopy. Cells were fixed, permeabilized, and probed with an mAb, OKT8, directed against the extracellular domain of CD8 (mAb anti-CD8; *A*). Binding of anti-CD8 antibody was determined with Texas red-labeled goat anti-mouse IgG. Two cells expressing the CD8/gp(TM + CT) chimera are shown in *A*. The focal plane is positioned to show the nuclear surface of one cell and the nuclear rim of the other. The locations of pore complexes within the same cells were identified using FITC-labeled mAb 414 (*C*). Those cells not expressing the chimeric protein are recognized only by mAb 414. Note the extensive coincidental staining at the nuclear surface and in the cytoplasm when comparing *A* and *C*. For comparison, the cell-surface expression of wild-type CD8 in 3T3 cells is shown in *B*. Bar, 10 μm.

by signal- and stop-transfer sequence–mediated mechanisms (14, 17). After integration into the ER membrane, sorting determinants specify retention within the ER or various downstream membranes of the exo- and endocytotic pathways (3). For the few examples of resident integral ER proteins that have so far been examined, COOH-terminal and, generally, cytoplasmically exposed regions, have been shown to be sorting determinants for their retention in the ER (13, 24, 26, 32). In this paper we have analyzed determinants that sort gp210 to a subdomain of the ER, the pore membrane domain of the NE. As the pore membrane is continuous with the ER, sorting to this domain is likely to proceed by lateral diffusion in the plane of the membrane rather than by vesicular traffic. gp210 is a bitopic integral membrane protein with a large NH_2-terminal cisternal domain (1,783 residues), a single TM, and a short COOH-terminal CT of 58 residues. The latter is topologically poised to interact with the NPC and a priori appeared to be the most likely candidate to harbor the determinant for sorting to the pore membrane. Surprisingly, we found that the TM of gp210 is sufficient for sorting to the pore membrane. Although the CT, particularly its COOH-terminal 20 residues, also contained a determinant for sorting to the pore membrane, the TM appeared to be the dominant sorting determinant. By itself, it was sufficient for sorting to the pore membrane. The ectoplasmic domain of gp210 that contributes 95% of its mass does not appear to contain determinants for sorting to the pore membrane. It appears to be retained in the ER, but our data do not rule out secretion.

In thinking about possible mechanisms by which the TM of gp210 could function as a dominant sorting determinant, one should consider the following uncertainties. First, the gp210 mutants studied here were expressed in cells that make their own "endogenous" gp210. We do not know the ratio of expressed (mutant) versus endogenous (wild-type) gp210 in individual pores. Second, although nuclear pores are doubled in S phase (22), mutant gp210 expression, over a period of 5 h, was assayed in unsynchronized, interphase cells. Thus, expressed mutant gp210 may have been involved in de novo formation of pores and/or may have gained ac-

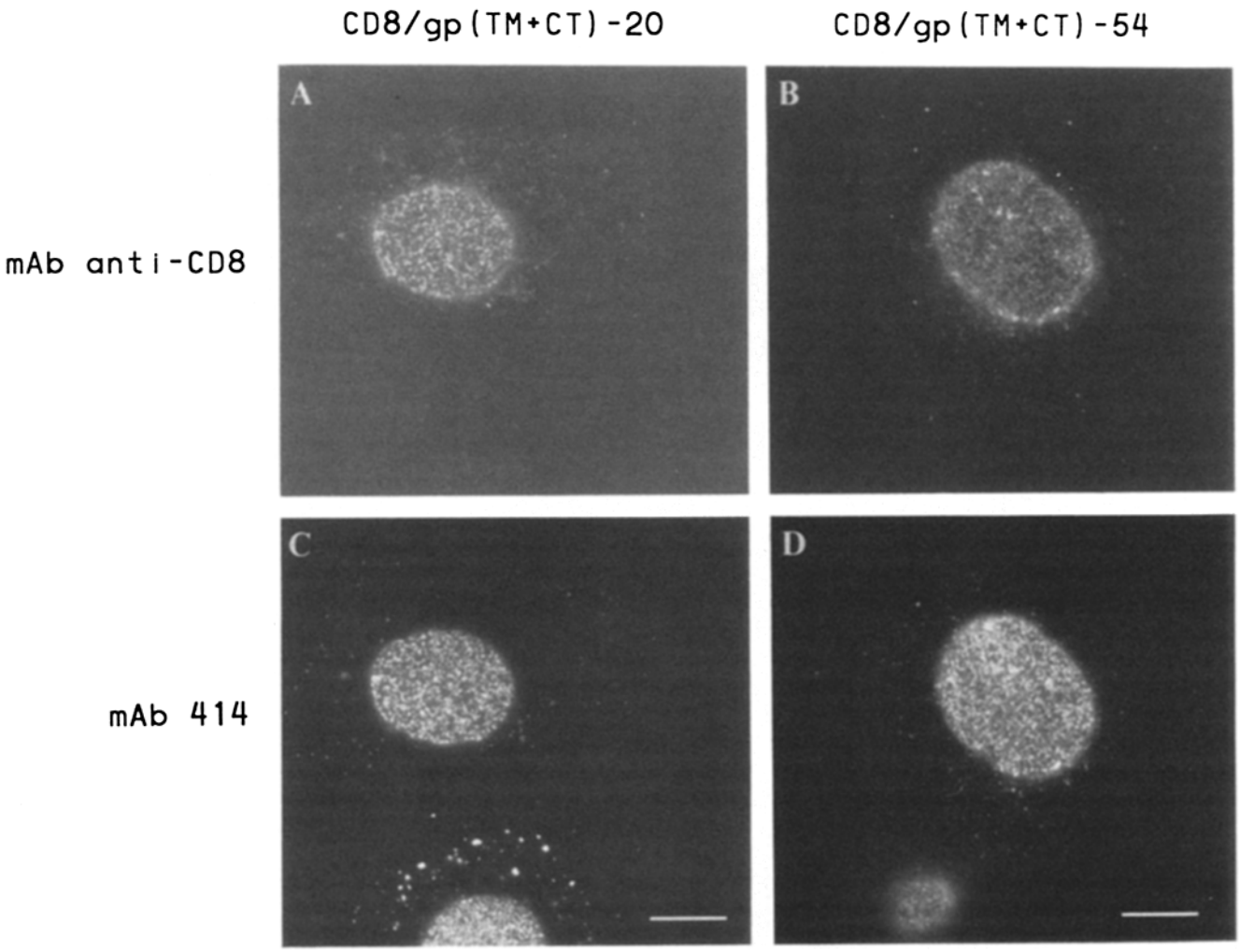

Figure 5. Targeting to the pore membrane of the CD8/gp(TM + CT) fusion protein is unaffected by deletions of the CT. 3T3 cells expressing the COOH-terminal deletion mutant CD8/gp(TM + CT)-20 or CD8/gp(TM + CT)-54 (see Fig. 1) were examined using the procedure described in Fig. 4 to visualize the chimeric proteins (*mAb anti-CD8*; *A* and *B*) and the pore complexes (*mAb 414*; *C* and *D*). All cells are recognized by mAb 414 (*C* and *D*), whereas only those expressing the chimeric proteins are detected with the anti-CD8 antibody (*A* and *B*). Bar, 10 μm.

cess to already formed pores by exchange with endogenous gp210. It should be noted that at present little is known about the dynamics of pore formation and NPC assembly or the stability of the interacting components. Whether involved in de novo formation of pores or in lateral exchange, we suggest that gp210's TM functions as the dominant sorting determinant because of the specific surface features of the α-helix that it forms. These features would allow specific lateral interactions with another transmembrane α-helix, either of gp210 or another integral membrane protein, to form a homodimer or heterodimer, respectively.

That lateral interactions between α-helices of TMs of integral membrane proteins can be specific was first demonstrated for the dimer of human erythrocyte glycophorin A (4, 16). Disruption of the dimer can be accomplished with a synthetic peptide representing the TM of glycophorin A but not with similar peptides representing the TMs of other integral membrane proteins (4, 16). Limited mutational analysis of this interaction suggests that close packing of side chains at the interface of adjacent helices may be required for dimerization (for a review of other examples of specific interactions via transmembrane helices see reference 16).

The TM of gp210 does not contain charged residues; thus, dimerization stabilized by charged ion pairs can be ruled out. It is noteworthy that the aromatic residues, two tyrosines and four phenylalanines, are arranged on one face of the membrane helix, with five of the six aromatic residues located on the NH_2-terminal half of the α-helix embedded into the cisternal leaflet of the pore membrane bilayer. Whether these or other features of the gp210 transmembrane α-helix allow specific lateral interactions with another transmembrane α-helix remains to be investigated.

There are precedents for TMs serving as topogenic determinants. Most resident integral proteins of the Golgi membrane that have so far been analyzed are retained there by sorting determinants in their TMs (20, 23, 25, 28, 33, 35, for review see 19).

The sorting determinants in gp210's CT, albeit apparently weaker than those of the TM, are likely to be relevant. If gp210 were to form homodimers via the TM, this could spa-

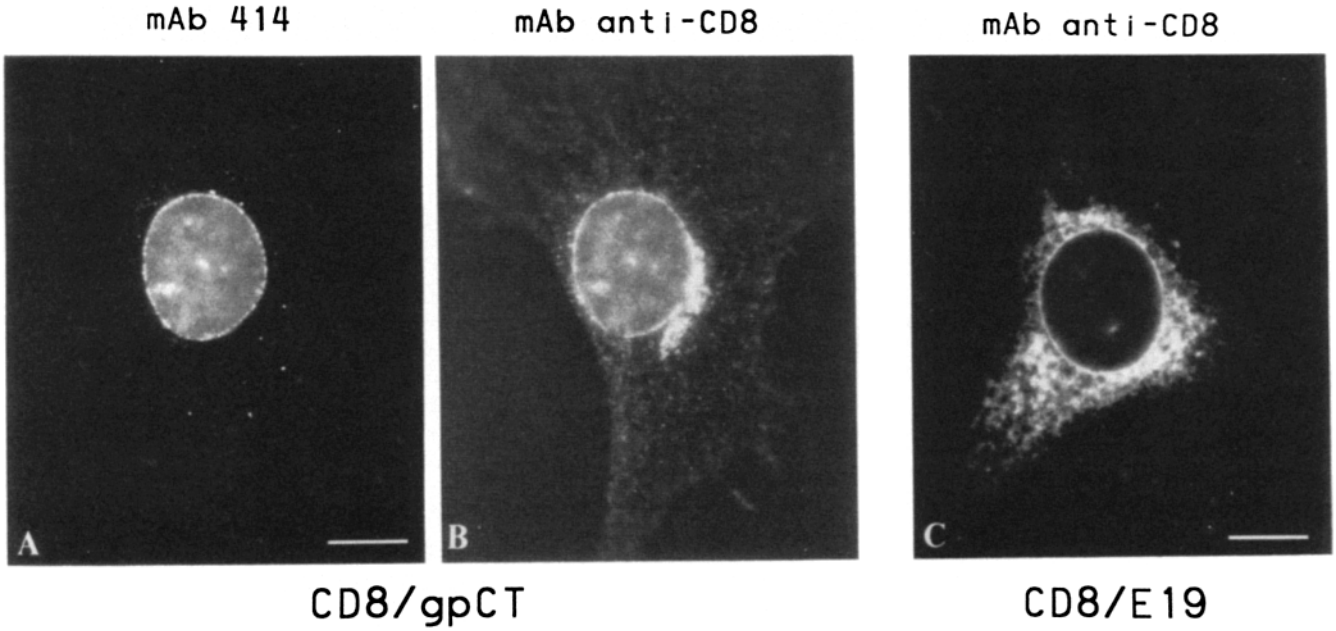

Figure 6. The CT of gp210 also contains a pore membrane targeting signal. The chimeric protein CD8/gpCT (see Fig. 1) was expressed in 3T3 cells and double immunofluorescence was performed, as described in Fig. 4, to visualize the chimeric protein (*mAb anti-CD8, B*) and pore complexes (*mAb 414, A*). Also shown is the distribution pattern of the CD8/E19 chimeric protein within a separate cell (*C*). In all cases, the focal plane shown passes through the center of the nucleus. In focus are the nuclear rim, adjacent regions of the cytoplasm, and portions of the plasma membrane. Note the presence of CD8/gpCT (*B*) at the cell surface as well as at the NE in a pattern similar to that revealed with mAb 414 (*A*). This distribution is compared to the CD8/E19 protein which is retained within the ER network and the NE (*C*). Bar, 10 μm.

tially orient the two CTs and give rise to cooperative binding effects to the NPC of significantly higher avidity than would be observed with a single CT alone. If gp210 were to form a heterodimer, a high affinity for the NPC of the CT of its heterodimeric partner could likewise result in cooperative binding effects of gp210's CT.

Our observation that a fraction of gp210 co-localizes with the cytoplasmically dispersed, mAb 414-reactive nucleoporins suggests that these components are associated with each other, perhaps in annulate lamellae. These structures are likely to represent excess pore membrane and pore complex components. Mutant gp210 appeared to be sorted to these

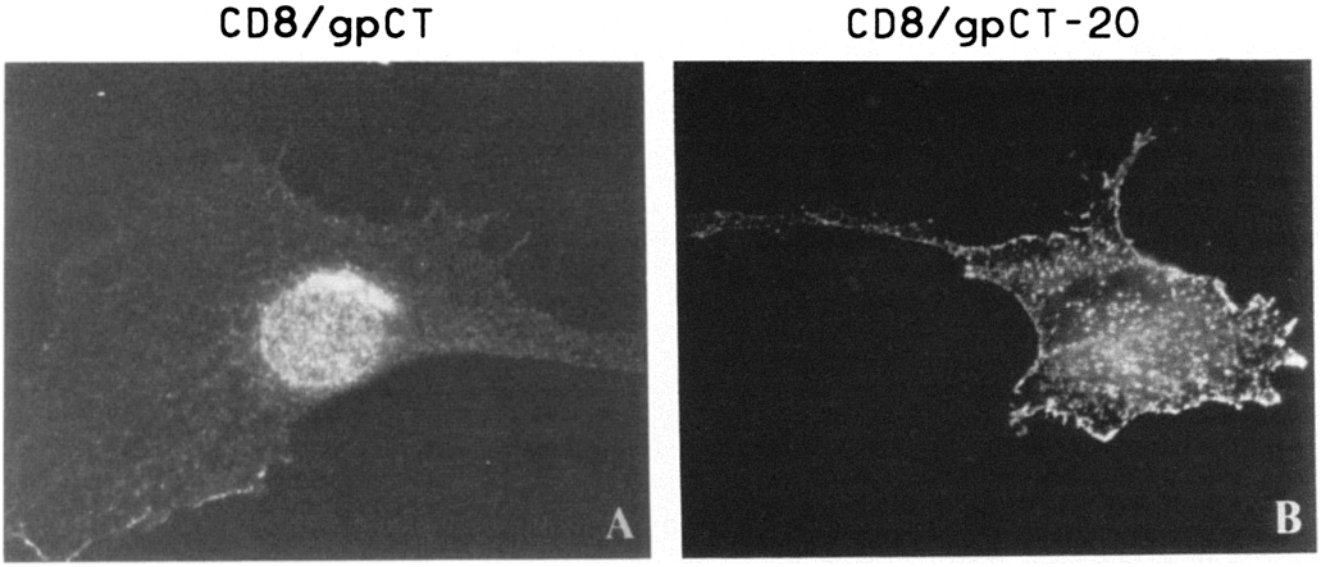

Figure 7. A 20-amino acid residue deletion from the COOH-terminal tail of the CD8/gpCT chimera abolishes NE localization. 3T3 cells expressing CD8/gpCT (*A*) or the deletion mutant CD8/gpCT-20 (*B*) were fixed, permeabilized, and probed with anti-CD8 antibody. Binding was visualized with Texas red-labeled goat anti-mouse IgG. The focal plane shown reveals the cell surface adjacent to the coverslip. Note that both chimeric proteins are visible at the cell surface (*A* and *B*), but the punctate NE staining pattern seen with CD8/gpCT (*A*) is absent in the CD8/gpCT-20 expressing cell (*B*). Bar, 10 μm.

cytoplasmic structures as long as they are also sorted to the pore membrane domain of the NE (see Figs. 2, 4, and 5). It therefore seems likely that sorting of gp210 to a pore membrane domain in the ER occurs by the same principles as sorting to the pore membrane domain of the NE.

This paper is dedicated to George E. Palade.

We wish to thank the Rockefeller University/Howard Hughes Medical Institute Biopolymer Facility for oligonucleotide synthesis; Drs. Christopher Nicchitta and Aurelian Radu for critical reading of the manuscript; and Drs. Eckart Bartnik, Giovanni Migliaccio, and Jean-Claude Courvalin for helpful discussion.

Received for publication 16 June 1992 and in revised form 8 September 1992.

References

1. Bailer, S. M., H. M. Eppenberger, G. Griffiths, and E. A. Nigg. 1991. Characterization of a 54-kD protein of the inner nuclear membrane: Evidence for cell cycle-dependent interaction with the nuclear lamina. *J. Cell Biol.* 114:389–400.
2. Berrios, M., A. J. Filson, G. Blobel, and P. A. Fisher. 1983. A 174 kDa ATPase/dATPase polypeptide and a glycoprotein of apparently identical molecular weight are common but distinct components of higher eukaryotic nuclear structural protein subfractions. *J. Biol. Chem.* 258:13384–13390.
3. Blobel, G. (1980). Intracellular protein topogenesis. *Proc. Natl. Acad. Sci. USA.* 77:1496–1500.
4. Bormann, B.-J., W. J. Knowles, and V. T. Marchesi. 1989. Synthetic peptides mimic the assembly of transmembrane glycoproteins. *J. Biol. Chem.* 264:4033–4037.
5. Capecchi, M. R. 1980. High efficiency transformation by direct microinjection of DNA into cultured mammalian cells. *Cell.* 22:479–488.
6. Courvalin, J.-C., K. Lassoued, E. Bartnik, G. Blobel, and R. W. Wozniak. 1990. The 210-kD nuclear envelope polypeptide recognized by human autoantibodies in primary biliary cirrhosis is the major glycoprotein of the nuclear pore. *J. Clin. Invest.* 86:279–285.
7. Davis, L. I., and G. Blobel. 1986. Identification and characterization of a nuclear pore complex protein. *Cell.* 45:699–709.
8. Field, J., J. Nikawa, D. Broek, B. MacDonald, L. Rodgers, I. A. Wilson, R. A. Lerner, and M. Wigler. 1988. Purification of a *ras*-responsive adenylyl cyclase complex from *Saccharomyces cerevisiae* by use of an epitope addition method. *Mol. Cell Biol.* 8:2159–2165.
9. Gerace, L., and B. Burke. 1988. Functional organization of the nuclear envelope. *Annu. Rev. Cell Biol.* 4:336–374.
10. Gerace, L., Y. Ottaviano, and C. Kondor-Koch. 1982. Identification of a major protein of the nuclear pore complex. *J. Cell Biol.* 95:826–837.
11. Greber, U. F., A. Senior, and L. Gerace. 1990. A major glycoprotein of the nuclear pore complex is a membrane-spanning polypeptide with a large lumenal domain and a small cytoplasmic tail. *EMBO (Eur. Mol. Biol. Organ.) J.* 9:1495–1502.
12. Franke, W. W. 1974. Structure, biochemistry and functions of the nuclear envelope. *Int. Rev. Cytol. Suppl.* 4:71–236.
13. Jackson, M. R., T. Nilsson, and P. A. Peterson. 1990. Identification of a consensus motif for retention of transmembrane proteins in the endoplasmic reticulum. *EMBO (Eur. Mol. Biol. Organ.) J.* 9:3153–3162.
14. Katz, F. N., J. E. Rothman, V. R. Lingappa, G. Blobel, and H. Lodish. 1977. Membrane assembly in vitro: synthesis, glycosylation, and asymmetric insertion of a transmembrane protein. *Proc. Natl. Acad. Sci. USA.* 74:3278–3282.
15. Kessel, R. 1983. The structure and function of annulate lamellae: porous cytoplasmic and intranuclear membranes. *Int. Rev. Cytol.* 82:181–304.
16. Lemmon, M. A., J. M. Flanagan, J. F. Hunt, B. D. Adair, B.-J. Bormann, C. E. Dempsey, and D. M. Engelman. 1992. Glycophorin A dimerization is driven by specific interactions between transmembrane α-helices. *J. Biol. Chem.* 267:7683–7689.
17. Lingappa V. R., F. N. Katz, H. F. Lodish, and G. Blobel. 1978. A signal sequence for the insertion of a transmembrane glycoprotein: Similarities to the signals of secretory proteins in primary structure and function. *J. Biol. Chem.* 253:8667–8670.
18. Littman, D. R., Y. Thomas, P. J. Maddon, L. Chess, and R. Axel. 1985. The isolation and sequence of the gene encoding T8: A molecule defining functional classes of T lymphocytes. *Cell.* 40:237–246.
19. Machamer, C. E. 1991. Golgi retention signals: Do membranes hold the key? *Trends Cell Biol.* 1:141–144.
20. Machamer, C. E., and J. K. Rose. 1987. A specific transmembrane domain of a coronavirus E1 glycoprotein is required for its retention in the Golgi region. *J. Cell Biol.* 105:1205–1214.
21. Maul, G. G. 1977. The nuclear and cytoplasmic pore complex. Structure, dynamics, distribution, and evolution. *Int. Rev. Cytol. Suppl.* 6:76–186.
22. Maul, G. G., H. M. Maul, J. E. Scogna, M. W. Lieberman, B. S. Stein, B. Y. Hsu, and T. W. Borun. 1972. Time sequence of nuclear pore formation in phytohemagglutinin-stimulated lymphocytes and in HeLa cells during the cell cycle. *J. Cell Biol.* 55:433–447.
23. Munro, S. 1991. Sequences within and adjacent to the transmembrane segment of α-2,6-sialyltransferase specify Golgi retention. *EMBO (Eur. Mol. Biol. Organ.) J.* 10:3577–3588.
24. Nilsson, T., M. Jackson, and P. A. Peterson. 1989. Short cytoplasmic sequences serve as retention signals for transmembrane proteins in the endoplasmic reticulum. *Cell.* 58:707–718.
25. Nilsson, T., J. M. Lococq, D. Mackay, and G. Warren. 1991. The membrane spanning domain of β-1,4-galactosyltransferase specifies *trans*-Golgi localization. *EMBO (Eur. Mol. Biol. Organ.) J.* 10:3567–3575.
26. Pääbo, S., B. M. Bhat, W. S. M. Wold, and P. A. Peterson. 1987. A short sequence in the COOH-terminus makes an adenovirus membrane glycoprotein a resident of the endoplasmic reticulum. *Cell.* 50:311–317.
27. Reinherz, E. L., and S. F. Schlossman. 1980. The differentiation and function in human T lymphocytes. *Cell.* 19:821–827.
28. Russo, R. N., N. L. Shaper, D. J. Taatjes, and J. H. Shaper. 1992. β-1,4-galactosyltransferase: A short NH_2-terminal fragment that includes the cytoplasmic and transmembrane domain is sufficient for Golgi retention. *J. Biol. Chem.* 267:9241–9247.
29. Senior, A., and L. Gerace. 1988. Integral membrane proteins specific to the inner nuclear membrane and associated with the nuclear lamina. *J. Cell Biol.* 107:2029–2036.
30. Severinsson, L., and P. A. Peterson. 1985. Abrogation of cell surface expression of human class 1 transplantation antigens by an adenovirus protein in *Xenopus laevis* oocytes. *J. Cell Biol.* 101:540–547.
31. Sukhatme, V. P., K. C. Sizer, A. C. Vollmer, T. Hunkapiller, and J. R. Parnes. 1985. The T cell differentiation antigen Leu-2/T8 is homologous to immunoglobulin and T cell receptor variable regions. *Cell.* 40:591–597.
32. Sweet, D. J., and H. R. B. Pelham. 1992. The *Saccharomyces cerevisiae* SEC20 gene encodes a membrane glycoprotein which is sorted by the HDEL retrieval system. *EMBO (Eur. Mol. Biol. Organ.) J.* 11:423–432.
33. Swift, A. M., and C. E. Machamer. 1991. A Golgi retention signal in a membrane-spanning domain of coronavirus El protein. *J. Cell Biol.* 115:19–30.
34. Wilson, I. A., H. L. Niman, R. A. Houghten, A. R. Cherenson, M. L. Connolly, and R. A. Lerner. 1984. The structure of an antigenic determinant in a protein. *Cell.* 37:767–778.
35. Wong, S. H., S. H. Low, and W. Hong. 1992. The 17-residue transmembrane domain of β-galactoside α-2,6-sialyltransferase is sufficient for Golgi retention. *J. Cell Biol.* 117:245–258.
36. Worman, H. J., J. Yuan, G. Blobel, and S. D. Georgatos. 1988. A lamin B receptor in the nuclear envelope. *Proc. Natl. Acad. Sci. USA.* 85:8531–8534.
37. Wozniak, R. W., E. Bartnik, and G. Blobel. 1989. Primary structure analysis of an integral membrane glycoprotein of the nuclear pore. *J. Cell Biol.* 108:2083–2092.